On climate response to changes in the cosmic ray flux and radiative budget

Nir J. Shaviv

Racah Institute of Physics, Hebrew University of Jerusalem, Jerusalem, Israel

[1] We examine the results linking cosmic ray flux (CRF) variations to global climate change. We then proceed to study various periods over which there are estimates for the radiative forcing, temperature change and CRF variations relative to today. These include the Phanerozoic as a whole, the Cretaceous, the Eocene, the Last Glacial Maximum, the 20th century, as well as the 11-yr solar cycle. This enables us to place quantitative limits on climate sensitivity to both changes in the CRF, and the radiative budget, F, under equilibrium. Under the assumption that the CRF is indeed a climate driver, the sensitivity to variations in the globally averaged relative change in the tropospheric ionization $\mathcal{I}$ is consistently fitted with $\mu \equiv -(dT_{global}/d\mathcal{I}) \approx 7.5 \pm 2°$K. Additionally, the sensitivity to radiative forcing changes is $\lambda \equiv dT_{global}/dF = 0.35 \pm 0.09°$KW^{-1}m^2, at the current temperature, while its temperature derivative is undetectable with $(d\lambda/dT)_0 = -0.01 \pm 0.04$ m^{2}W^{-1}. If the observed CRF/climate link is ignored, the best sensitivity obtained is $\lambda = 0.54 \pm 0.12°$KW^{-1}m^2 and $(d\lambda/dT)_0 = -0.02 \pm 0.05$ m^{2}W^{-1}. Note that this analysis assumes that different climate conditions can be described with at most a linear function of T; however, the exact sensitivity probably depends on various additional factors. Moreover, λ was mostly obtained through comparison of climate states notably different from each other, and thus only describes an average sensitivity. Subject to the above caveats and those described in the text, the CRF/climate link therefore implies that the increased solar luminosity and reduced CRF over the previous century should have contributed a warming of $0.47 \pm 0.19°$K, while the rest should be mainly attributed to anthropogenic causes. Without any effect of cosmic rays, the increase in solar luminosity would correspond to an increased temperature of $0.16 \pm 0.04°$K.

1. Introduction

[2] Accumulating evidence suggests that solar activity is responsible for at least some climatic variability. These include correlations between solar activity and either direct climatic variables or indirect climate proxies over time scales ranging from days to millennia [*Herschel*, 1796; *Eddy*, 1976; *Labitzke and van Loon*, 1992; *Friis-Christensen and Lanssen*, 1991; *Soon et al.*, 1996a, 2000; *Beer et al.*, 2000; *Hodell et al.*, 2001; *Neff et al.*, 2001]. It is therefore difficult at this point to argue against the existence of any causal link between solar activity and climate on Earth. However, the climatic variability attributable to solar activity is larger than could be expected from the typical 0.1% changes in the solar irradiance observed over the decadal to centennial time scale [*Beer et al.* 2000; *Soon et al.*, 2000]. Thus, an amplifier is required unless the sensitivity to changes in the radiative forcing is uncomfortably high.

[3] The first suggestion for an amplifier of solar activity was suggested by Ney, who pointed out that if climate is sensitive to the amount of tropospheric ionization, it would also be sensitive to solar activity since the solar wind modulates the cosmic ray flux (CRF), and with it, the amount of tropospheric ionization [*Ney*, 1959].

[4] Over the solar cycle, the interplanetary magnetic field varies considerably, such that the amount of tropospheric ionization changes by typically 5%. *Svensmark* [1998, 2000], *Marsh and Svensmark* [2000a] as well as *Palle Bago and Butler* [2000] have shown that the variations in the amount of low altitude cloud cover (LACC) nicely correlate with the CRF reaching Earth over two decades. A recent analysis has shown that the latitudinal variations of the LACC are proportional to the latitudinal dependence of the low altitude ion concentrations [*Usoskin et al.*, 2004a]. This suggests that it is more likely that the cloud cover is directly related to the CRF than directly to solar activity.

[5] More recent data on the LACC seems to exhibit a weaker correlation with the variable CRF [e.g., *Farrar*, 2000]. There are however a few peculiarities in the data

which are indicative of a calibration problem, which once removed, seem to recover the high correlation between the CRF and the LACC [*Marsh and Svensmark*, 2003]. For an objective review, the reader is encouraged to read *Carslaw et al.* [2002].

[6] The above correlations between CRF variability and climate (and in particular, cloud cover), indicate that CRF modulations appear to be responsible for climate variability, most probably through modulation of the amount of LACC. Nevertheless, since all of the above CRF variability ultimately originates from solar activity changes, it is not possible to unequivocally rule out the possibility that the CRF/climate correlations are coincidental, and that both are independently modulated by solar activity with similar lags.

[7] An independent CRF/climate correlation on a much longer time scale, in which variations in the CRF do not originate from solar variability, was found by *Shaviv* [2002a, 2002b] and *Shaviv and Veizer* [2003]. It was shown using astronomical data that the CRF should change by more than a factor of 2 because of our passages through the galactic spiral arms, with a period of 132 ± 25 Ma [*Shaviv*, 2002b]. It was also shown that the CRF history can actually be reconstructed using the cosmic-ray exposure age data of Iron meteorites, exhibiting a periodicity of 143 ± 10 Ma and a phase consistent with the astronomical data. Moreover, it was found that the reconstructed CRF nicely synchronizes to the occurrence of ice-age epochs on Earth, which appeared on average every 145 ± 7 Ma over the past billion years. Additionally, the mid-point of the ice-age epochs is predicted to lag by 31 ± 8 Ma after the mid-point of the spiral arm crossing, while it is observed to lag by 33 ± 20 Ma. That is, the CRF and ice-age epoch signals agree in both phase and period. The same analysis also revealed that the long term star-formation activity of the Milky Way correlates with long term glacial activity on Earth. In particular, a dearth in star formation between 1 and 2 Ga before present, coincides with a long period during which glaciations appear to have been totally absent [*Shaviv*, 2002b, 2003].

[8] We should also point out several experimental results supporting, though not proving yet, a CRF/cloud cover link. *Harrison and Aplin* [2001] found experimentally that CN formation is correlated with natural Poisson variability in cosmic ray showers. In other words, this link appears to be more than hypothetical. In another set of experiments, it was shown that cosmic rays play a decisive role in the formation of small clusters [*Eichkorn et al.*, 2002]. If these small clusters can be shown to grow quickly enough, as opposed to being scavenged by large particles, the link between cosmic rays and the formation of cloud condensation nuclei and ultimately cloud cover could be firmly established.

[9] We will not dwell here on the actual mechanism responsible for CRF link with cloud behavior. We will simply assume henceforth that this link exists, as supported by empirical and experimental data, even though it is still an issue of debate. This point has to be kept in mind since the conclusions we shall reach, will only be valid if this assumption is correct.

[10] Using the above assumption, we study several time scales to see whether estimates on global temperature sensitivity can be placed, together with estimates on the

CRF/temperature relation. We will do so by comparing the observed temperature changes with changes in the radiative budget, an approach previously pursued in numerous analyses [e.g., *Hoffert and Covey*, 1992; *Covey et al.*, 1996; *Hansen et al.*, 1993; *Gregory et al.*, 2002]. This method for obtaining the global temperature sensitivity using paleodata is orthogonal to the usage of global circulation models (GCMs) upon which often quoted results are based [*IPCC* 2001]. Hence, the two methods suffer from altogether different errors. It is therefore clearly advantageous to follow this path as an independent estimate. For example, *Cess et al.* [1989] have shown that the large uncertainty in the sensitivity obtained in GCMs stems from the uncertain feedback of cloud cover. Since we use the actual global data, all the feedbacks are implicitly considered. The main contribution in this work is to specifically consider the contribution of the CRF to the changed radiative budget. As a note of caution, one should keep in mind that the most notable assumption in this method is the quantification of climate sensitivity with one number. In other words, it assumes that on average Earth's climate responds the same irrespective of the geographic, temporal or frequency space distribution of the radiation budget changes. It also assumes that different radiative forcings act linearly.

[11] Once the radiative forcing and temperature changes are obtained, the sensitivities can be estimated with

$$\lambda \equiv \frac{dT_{global}}{dF}\bigg|_{F=F_0} \approx \frac{\Delta T}{\Delta F}. \qquad (1)$$

ΔF, which is the globally averaged change in the radiation flux (per unit surface area), will also include here the contribution ΔF_{CRF} arising from a changed energy flux ϕ of cosmic rays. Note also that over short time scales, ΔT or ΔF have to be properly modified to include the finite heat capacity of the system, and the consequent finite adjustment time it has. We should also consider the possibility that λ is dependent on the temperature. For example, the positive climate feedback arising from the formation of ice sheets could increase the sensitivity of a glaciated Earth, while the reduced atmospheric water vapor content, can reduce the sensitivity.

[12] In addition to λ, we will also estimate the sensitivity to CRF variations, or more specifically, to changes in the global atmospheric ion density.

2. Radiative Forcing of Low Altitude Cloud Cover

[13] Without a detailed physical model for the effects of cosmic rays on clouds or a detailed enough record of radiation budget measurements correlated with the solar cycle, it is hard to accurately determine the quantitative link between CRF variations and changes in the global radiation budget. In particular, it is hard to do so without limiting ourselves to various approximations. Nevertheless, this link is important since it will be used in most of our estimates for the global temperature sensitivity.

[14] The basic observation we use to estimate the radiative forcing of clouds is the apparent correlation between CRF variations and the amount of low altitude cloud cover.

A naive approximation is to assume that the whole climatic effect can be described by variations in the extent of the cloud cover, namely, that we neglect effects in the cloud properties, or possible climatic effects associated with atmospheric ionization but not with clouds. It also implies that the geographical distribution of the effect is the same as low altitude clouds on average. We will first estimate this "zeroth" order term and then try to estimate the possible contribution of other corrections.

[15] Amount of cloud cover: Over the solar cycle, the varying CRF appears to cause a 1.2 to 2.0% (absolute) change in the amount of LACC [*Marsh and Svensmark*, 2000b; *Kirkby and Laaksonen*, 2000; *Marsden and Lingenfelter*, 2003; *Carslaw et al.*, 2002]. We will therefore adopt a change of 1.6 ± 0.4% in the LACC.

[16] The total radiative forcing of the LACC is estimated to be −16.7 Wm^{-2} from the average 26.6% cloud cover [*Hartmann et al.*, 1992]. If one however compares the forcing of the total cloud cover from different hemispheres and different experiments (Nimbus and ERBE [*Ardanuy et al.*, 1991]), one finds variations which are typically 2.5 Wm^{-2} on the ∼50 Wm^{-2} shortwave (SW) "cooling" and 7 Wm^{-2} on the 27 Wm^{-2} longwave (LW) "warming". Since LACC typically comprise half of the total amount cloud cover, an error of ∼4 Wm^{-2} is to be expected.

[17] Thus, the changed radiative forcing ΔF_f associated with the varying amount of cloud cover, should be −1.0 ± 0.35 Wm^{-2}. This implicitly assumes that the incremental cloud cover has the same average net radiative properties as the whole 27% of the LACC.

[18] Cloud optical depth: Changes in the cloud properties could take place in addition to changes in the cloud amount. According to *Marsden and Lingenfelter* [2003], there is a small negative correlation between the average LACC opacity $\bar{\tau}$ and the varying CRF. Over the solar cycle, $\bar{\tau}$ changes by −4% relative to its global average of about 4 in regions defined to be covered by LACC.

[19] Is such a change in $\bar{\tau}$ reasonable? According to *Marsden and Lingenfelter* [2003], there are two limiting cases for the effects on cloud properties. The first is changing the number density of cloud condensation nuclei (CCN) given a fixed amount of Liquid Water Content (LWC), that is, CCN limited. This is similar to the "Twomey effect" where enhanced aerosol density affects the droplet size and cloud albedo [*Twomey*, 1977; *Rosenfeld*, 2000]. The second case is increasing the CCN density together with the LWC, and obtaining similar sized drops (LWC limited). Although the two cases are plausible, they do not change the cloud properties in the same way.

[20] One can show that a cloud's optical depth for SW absorption is [e.g., *Marsden and Lingenfelter*, 2003]

$$\tau \approx \frac{3}{2} \frac{\rho_{\text{eff}} \Delta z}{\rho_0 R_{\text{eff}}}, \qquad (2)$$

where ρ_0 is the density of water, ρ_{eff} is the mass loading of water (i.e., its effective density), Δz is the vertical extent of the cloud and R_{eff} is the effective radius of the cloud droplets, defined as the ratio between the 3rd and 2nd moments of the droplet distribution ($\langle r^3 \rangle / \langle r^2 \rangle$). In the case of a CCN limited condensation, $R_{\text{eff}} \propto n_{CCN}^{-1/3}$, and τ will increase with n_{CCN}, while in the LWC limiting case,

$\rho_{\text{eff}} \propto n_{CCN}$ and τ will increase as well. One can therefore write:

$$\frac{\delta\tau}{\tau} = \beta \frac{\delta n_{CCN}}{n_{CCN}}, \qquad (3)$$

with $\beta = 1$ for LWC limited case and $\beta = 1/3$ for the CCN limited case. Since the lower troposphere ionization rate changes by about 7% between solar minimum and maximum, we should expect to get at most a similar increase in the CCN. Thus we should expect $\delta\tau/\tau \lesssim 7\%$. The fact that a negative change in τ was observed [*Marsden and Lingenfelter*, 2003], could arise because the increase in cloud lifetime results with thinner clouds on average.

[21] Next, one can approximate the relation between τ and cloud albedo $\mathcal{A}$, by the relation [*Hobbs*, 1993]:

$$\mathcal{A} \approx \frac{\tau}{\tau + \tau_{1/2}}, \qquad (4)$$

where $\tau_{1/2} \approx 6.7$ for an asymmetry parameter of 0.85 [*Hobbs*, 1993]. Once we differentiate, we find:

$$\frac{d\mathcal{A}}{d\tau} \approx \frac{\mathcal{A}^2 \tau_{1/2}}{\tau^2}. \qquad (5)$$

If we consider the transmission $\mathcal{T} \approx 0.75$ of the atmosphere (to obtain a top-of-atmosphere albedo, from a cloud-top albedo), that the LACC covers only a fraction f_{low} of the globe, and that the average top-of-atmosphere incidence of radiation is $\bar{F} = 344$ Wm^{-2}, we find that the change in albedo is responsible for a changed radiation budget of

$$\Delta F_{\mathcal{A}} \approx \frac{\mathcal{A}^2 \tau_{1/2}}{\tau^2} \bar{F} \mathcal{T}^2 f_{low} \delta\bar{\tau} \approx +0.13 \text{Wm}^{-2}. \qquad (6)$$

The positive sign implies that the small apparent reduction in $\bar{\tau}$ contributes a small warming contribution.

[22] If we had no knowledge of $\bar{\tau}$, changes in it could have resulted with a correction to $\Delta F_{\mathcal{A}}$ which are only as large as −0.23 Wm^{-2} (for the LWC limited case, and $\delta\tau/\tau \lesssim 7\%$). We take this uncertainly in $\bar{\tau}$ as another source of error for the radiative forcing ΔF.

[23] Cloud emissivity: There could still be more physical terms contributing to ΔF. If the LWC in the clouds can vary as well (that is, the clouds are not CCN limited but rather water limited), then also the IR emissivity can change. It will do so by changing the emissivity, relative to black body [e.g., *Stephens*, 1978] which is given by

$$\epsilon(\Delta z) = 1 - \exp(-\tau_{IR}). \qquad (7)$$

where we have defined $\tau_{IR} \equiv a_0 \rho_{\text{eff}} \Delta z$. Here, ρ_{eff} is the liquid water content, a_0 is the mass absorption coefficient (for water clouds, $a_0 \approx 0.13$ m^{2}g^{-1} [*Stephens*, 1978]) and δz is the thickness of the cloud layer above a given point. By changing the emissivity, we change the outgoing long-wavelength flux by

$$\Delta F_{IR} = \mathcal{T} \sigma T^4 f_{low} \Delta\epsilon = \exp(-\tau_{IR}) \mathcal{T} \sigma T^4 \tau_{IR} \frac{\Delta\rho_{\text{eff}}}{\rho_{\text{eff}}} \qquad (8)$$

where $\mathcal{T} \sim 0.6$ is the transmittance of the atmosphere to IR, above the cloud. For typically small values of ρ_{eff} of 0.3 g/m^3, and $\delta z = 100$ m (which would give the largest effect), we get corrections of $\Delta F_{IR} = 1.1$ Wm^{-2} $(\Delta\rho_{eff}/\rho_{eff}) \lesssim 0.1$ Wm^{-2}. This positive flux outwards tends to cool (i.e., increase the CRF/temperature effect), but it is a small effect.

[24] By changing the emissivity, we can also shift the apparent location of the top of the clouds, and with it their temperature. In other words, we should expect outgoing LW radiation to come from higher up the atmosphere where the temperature is lower.

[25] A higher ρ_{eff} will shift the IR emission "surface" vertically by typically:

$$\Delta z \sim \frac{1}{a_0 \rho_{eff}} \left(\frac{\Delta\rho_{eff}}{\rho_{eff}} \right). \qquad (9)$$

Using the black body law, the change in the radiative emission over the solar cycle will therefore be less than

$$-\Delta F_{\Delta T} \lesssim f_{low} 4\sigma T^3 \Delta z \frac{dT}{dz} \lesssim 0.2 \frac{\Delta\rho_{eff}}{\rho_{eff}} \text{Wm}^{-2}, \qquad (10)$$

once globally averaged. For the last inequality, we took a typically low ρ_{eff} of 0.3 g/m^3, a wet adiabat of $dT/dz \sim 0.6$°K $(100 \text{ m})^{-1}$ and $f_{low} \approx 0.28$. Since $\Delta\rho_{eff}/\rho_{eff} \lesssim 0.1$, this effect will be even smaller at best (and in opposite sign as the previous effect).

[26] This result is also reasonable considering that the total long wavelength heating effect of LACC was estimated to be ~ 3.5 Wm^{-2} [Hartmann et al., 1992], while cloud albedo is responsible for a globally averaged cooling of ~ 20 Wm^{-2}, implying that changes in albedo will likely be more important for changing the radiative budget arising from LACC variations.

[27] Ocean bias: Additional unaccounted effects are possible. For example, we implicitly assumed before that the effects of a changed LACC on the radiation budget can be described by the average effect of LACC. This would be the case if the geographic distribution of the LACC variations is the same as the distribution of the average LACC. This need not be the case. Specifically, we expect the CRF effect to be more dominant in marine environments, where CCN are relatively scarce. But the average radiative properties of LACC over oceans is different than the globally averaged properties of LACC. This is because covering or uncovering the ocean with clouds corresponds to a different change in the albedo than those arising from covering or uncovering land.

[28] Quantitatively, the Earth's albedo can be approximated with

$$\mathcal{A} = \alpha_l [f_l \mathcal{A}_c + (1 - f_l)\mathcal{A}_l] + \alpha_o [f_o \mathcal{A}_c + (1 - f_o)\mathcal{A}_o] \qquad (11)$$

where $\alpha_l \approx 1/3$ and $\alpha_o \approx 2/3$ are the surface fractions covered by land and oceans, respectively. $\mathcal{A}_c$ is the average cloud albedo, $\mathcal{A}_l$ and $\mathcal{A}_o$ are the average cloudless land and ocean albedos, while f_l and f_o are respectively the fractions of land and ocean covered with clouds.

[29] An unbiased LACC/CRF effect would change the total cloud cover while keeping fixed the ratio $r \equiv f_l/f_o \approx 0.5$.

If on the other hand all the LACC variations associated with a changed CRF are limited to the oceans, then f_l is kept fixed. The additional albedo change associated with the biased case, as compared with the unbiased case can be straightforwardly calculated to be $\Delta\mathcal{A} \approx (\mathcal{A}_l - \mathcal{A}_o)r (1 - \alpha_o)/(r + \alpha_o - r\alpha_o) \Delta f_{low} \sim 0.03 \Delta f_{low}$, where we have assumed $\mathcal{A}_l - \mathcal{A}_o \sim 15\%$. This corresponds to a flux change of $\Delta F_{\Delta\mathcal{A}} \approx \Delta\mathcal{A}\mathcal{T}^2 \bar{F} \approx +0.1$ Wm^{-2} over the solar cycle. That is, a likely ocean bias implies that we are slightly underestimating ΔF_{CRF}.

[30] Other effects: If the effect is geographically localized to certain areas, then a larger discrepancy could arise if the radiative properties of the LACC over those geographic regions is significantly different from the properties of LACC on average. A correlation map between LACC variations and CRF change [Marsh and Svensmark, 2000b], reveals that some regions (particularly over oceans) stand out with a higher correlation than others. Nevertheless, they do not appear to cluster around particular latitudes or other special regions. Thus, the assumption of geographic uniformity may be not that bad.

[31] Another hard to estimate effect could arise from the expected increase in cloud lifetime. For example, cumulus-type clouds could penetrate into higher altitudes, thereby reducing their IR emission.

[32] Thus, until we fully understand all the details in the physical picture, we should take the estimated radiative forcing and the error with a grain of salt. Taking the above into considerations, our best estimate for the radiative forcing of the cloud cover variations over the solar cycle is $\Delta F_{CRF} = \Delta F_f + \Delta F_\mathcal{A} + \Delta F_{\Delta\mathcal{A}} = 1.0 \pm 0.4$ Wm^{-2}, globally averaged (we have neglected $\Delta F_{IR} \lesssim 0.1$ Wm^{-2} and $-\Delta F_{\Delta T} \lesssim 0.02$ Wm^{-2}). This should be compared with the 0.1% solar flux variations, giving rise to an extra "direct" forcing of $\Delta F_{flux} \approx 0.35$ Wm^{-2} [Frohlich and Lean, 1998].

[33] Our goal here, is to find a number describing the relation between CRF variations and changes in the radiative forcing. However, instead of working with the CRF itself, we will work with $\mathcal{I}$, the cosmic ray induced ionization (CRII), which is the global average of the relative change in the atmospheric ion density. We do so, because, it was found empirically that the LACC change is linear in this value [Usoskin et al., 2004a]. This relation appears to hold even locally at given latitudinal bands. The CRII itself is proportional to the square root of the ionization rate, since the ion density is dominated by ion-ion recombination [Ermakov et al., 1997].

[34] Over the recent solar cycles, the solar modulation parameter $\Phi_\odot$ has changed between approximately 500 and 1000 MeV. Using the results of Appendix A, the CRII has changed by $\Delta\mathcal{I} \approx 4.5\%$.

[35] Thus, we find that the radiative sensitivity to CRF variations is about

$$\alpha \equiv -\frac{dF}{d\mathcal{I}} = 22 \pm 9 \text{Wm}^{-2}. \qquad (12)$$

3. Estimating Climate Sensitivity

[36] We now proceed to estimate the climate sensitivity. We do so by comparing the radiative forcing change
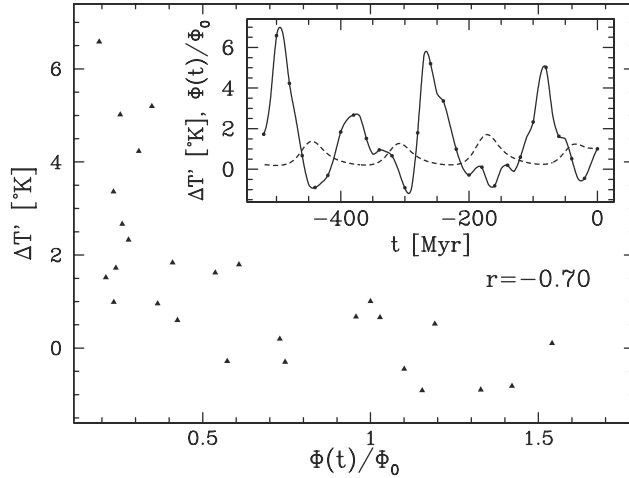
Figure 1. The high correlation between the reconstructed temperature and CRF over the Phanerozoic can be used to estimate global sensitivity. Here, $\Delta T'$ is the reconstructed temperature ΔT of *Veizer et al.* [2000] binned into 20 Myr bins, over the past 550 Ma, with a small linear temperature increase of $1.7°K$ ($t/550$ *Ma*) subtracted [see *Shaviv and Veizer*, 2003]. The CRF is one of 3 reconstructions used in *Shaviv and Veizer* [2003]. The two others differ in the total amplitude of variations. The two independent signals have a high Pearson correlation of $r = -0.70$. Although statistically significant limits on p cannot be placed, lower p values are favored (with $p \sim 0.3$ producing the best fit). Nevertheless, the value of $p = 0.5$ is theoretically preferred. The inset shows the time dependence of the two signals.

between two eras to the temperature change which ensued, using equation (1). In most estimates, we will rely on the results of section 2 to obtain the contribution of the changed CRF, and with it changes in the CRII, to the changed radiative forcing. These include seven different comparisons, spanning from variations over the solar cycles, to variations over the Phanerozoic as a whole. Subsequently, we will combine the results to obtain our best estimate for the climate sensitivity.

3.1. ΔT/CO$_2$ Correlation Over the Phanerozoic

[37] *Shaviv and Veizer* [2003] have shown that more than two thirds of the variance in the reconstructed tropical temperature variability ΔT_{trop} over the Phanerozoic can be explained using the variable CRF, which could be reconstructed using Iron meteorites. On the other hand, it was shown that the reconstructed atmospheric CO_2 variations do not appear to have any clear correlation with the reconstructed temperature. The large correlation between reconstructed CRF and temperature is seen in Figure 1. It is this correlation which led the authors to conclude that the Phanerozoic climate is primarily driven by a celestial driver. The lack of any apparent correlation with CO_2 was used to place a limit on the global climate sensitivity. This is because changes in the atmospheric CO_2 concentration imply changes to the earth radiative budget.

[38] A subsequent analysis by *Royer et al.* [2004] has shown that pH corrections could have been important at offsetting the $\delta^{18}O$ record upon which the temperature

reconstruction is based. In particular, The pH correction term of *Royer et al.* [2004] has the form:

$$\Delta T_{pH} = a\{\log R_{CO2} + \log \Lambda(t) - \log \Omega(t)\}, \quad (13)$$

where R_{CO2} is the atmospheric partial pressure of relative to today, $\Lambda(t)$ is $(Ca)(t)/(Ca)(0)$ - the mean concentration of dissolved calcium in the water relative to today, while $\Omega(t)$ is $[Ca^{++}][CO_3^{--}]/K_{sp}$ at time t relative to today. The expression for a essentially contains two factors. The first is a theoretically calculated factor characterizing the effect of pH on $\delta^{18}O$. The second is the translation between $\delta^{18}O$ and temperature variations. Once the ice-volume effect on $\delta^{18}O$ is considered [*Veizer et al.*, 2000; *Shaviv and Veizer*, 2004], one obtains: $a \approx 1.4°K$.

[39] Since the pH correction depends on R_{CO2}, so will the corrected temperature. A simple correlation between the corrected temperature and the reconstructed R_{CO2} will then be meaningless. Instead, the method to proceed is to defined a CO_2 "uncorrected" temperature as:

$$\Delta T' = \Delta T - a \log R_{CO2}. \quad (14)$$

Any correlation that this signal will have with R_{CO2} will then be real, since this "temperature" depends only on $\delta^{18}O$, and the small Λ and Ω terms. This uncorrected temperature can then be fitted with

$$\Delta T'_{model} = A + Bt + (C - a \log_{10} 2) \log_2 R_{CO2} + Dg[\phi(t)]. \quad (15)$$

A and B allow for systematic secular trends in the data. These arise from the well understood solar luminosity increase and the poorly understood tectonically controlled trend in the $\delta^{18}O$ data [*Veizer et al.*, 2000]. D relates the cosmic ray energy flux $\phi(t)$ to ΔT [*Shaviv and Veizer*, 2003]. The term $(a \log_{10} 2)$ $log_2 R_{CO2}$ was added such that C will keep its original meaning in *Shaviv and Veizer* [2003], which is the tropical temperature increase associated with a doubled R_{CO2}.

[40] This assumes that the radiative forcing is logarithmic in R_{CO2}, that is, that $\Delta F_{CO2} \approx \Delta F_{\times 2} \log_2 [R_{CO2}/(280 \text{ ppm})]$ and that over the entire range of the Phanerozoic, the temperature sensitivity to ΔF is constant. Over the order of magnitude variations in R_{CO2}, the former approximation is good to within 10% of actual calculations [*Hansen et al.*, 1998]. This is good enough considering the uncertainties in the second approximation, which does appears to be consistent with the data (see section 3.8.2). For the effect of a doubled CO_2 concentration, we take $\Delta F_{\times 2} = 3.71 \text{ Wm}^{-2}$ [*Myhre et al.*, 1998]. As for the CO_2 reconstruction itself, there are a few to choose from. The analysis described below uses the more common GEOCARB III reconstruction [*Berner and Kothavala*, 2001], but the limits obtained are actually insensitive to the preferred model [*Shaviv and Veizer*, 2003].

[41] The lack of a correlation between $\delta^{18}O$ and R_{CO2} [*Shaviv and Veizer*, 2003] originates from the fact that $(C - a \log_{10} 2)$ happens to be coincidentally close to 0. In other words, the pH correction to $\delta^{18}O$ and ΔT happens to be similar to the tropical temperature sensitivity to changes in R_{CO2}. (Without the pH correction, the preferred value for

Table 1. Limits on the Sensitivity of Global Temperature to Radiative Forcing, Using Different Methods While Assuming That CRF Does or Does Not Affect Climate[a]

Period (Method)	λ, °KW^{-1}m^2					$\Delta T_{\times 2}$,°K				
	1%	16%	50%	84%	99%	1%	16%	50%	84%	99%
Without the Effect of Cosmic Rays										
Phanerozoic (CO_2/T)	0.02	0.19	0.36	0.63	1.05	0.1	0.5	1.3	2.3	3.9
Cretaceous[b]	0.29	0.38	0.57	1.01	*[c]	1.1	1.4	2.1	3.8	*
Eocene[d]	0.03	0.21	0.37	0.56	0.87	0.1	0.8	1.4	2.1	3.3
LGM[d,e]	0.10	0.38	0.58	0.87	1.48	0.4	1.4	2.2	3.2	5.5
20th Century[f]	0.34	0.67	1.31	*	*	1.4	2.5	4.9	*	*
Solar Cycle	0.24	0.58	0.94	1.85	*	0.9	2.2	3.5	6.8	*
Combined (λ = *const*)	0.33	0.44	0.52	0.62	0.79	1.3	1.6	1.9	2.3	2.9
Combined ($\lambda = \lambda_0 + b\Delta T$)	0.24	0.43	0.54	0.66	0.87	0.9	1.6	2.0	2.5	3.2
With the Effect of Cosmic Rays										
Phanerozoic (CO_2/T)[g]	0.02	0.14	0.28	0.43	0.65	0.1	0.5	1.0	1.6	2.4
Phanerozoic (CRF/T)[h]	0.11	0.23	0.34	0.59	2.4	0.4	0.8	1.3	2.2	8.9
Phanerozoic (Clouds)[h,i]	0.2					0.8				
Cretaceous[b,h]	0.15	0.28	0.40	0.65	2.1	0.6	1.0	1.5	2.4	7.8
Eocene[d,h,j]	0.03	0.23	0.41	0.73	2.4	0.1	0.8	1.5	2.7	8.8
LGM (LACC)[d,e,h]	0.08	0.29	0.44	0.65	1.04	0.3	1.1	1.6	2.4	3.9
LGM (μ)[d,e,k]	0.04	0.28	0.48	0.75	1.30	0.2	1.0	1.8	2.8	4.8
20th Century[h]	0.09	0.17	0.27	0.59	*	0.3	0.6	1.0	2.2	*
Solar Cycles	0.07	0.15	0.26	0.52	2.10	0.2	0.6	1.0	1.9	7.8
Combined[j] (λ = *const*)	0.18	0.24	0.28	0.35	0.44	0.7	0.9	1.0	1.3	1.6
Combined[j] ($\lambda = \lambda_0 + b\Delta T$)	0.18	0.26	0.34	0.44	0.75	0.7	1.0	1.3	1.6	2.8

[a]$\Delta T_{\times 2}$ is caluclated using a forcing of 3.71 Wm^{-2} [*Myhre et al.*, 1998]. The columns denote the values below which λ (or $\Delta T_{\times 2}$) are expected to be found at the given probability, as obtained with the particular method, or, once the methods are combined, either by assuming λ is strictly constant, or by assuming it can vary linearly with temperature.
[b]Based on *Hoffert and Covey* [1992].
[c]Limits for $\Delta T_{\times 2}$ larger than 10°K are meaningless and therefore not quoted.
[d]Based on *Covey et al.* [1996].
[e]Based on *Hansen et al.* [1993].
[f]Based on *Gregory et al.* [2002].
[g]Based on *Shaviv and Veizer* [2003].
[h]Assumes the CRF-climate is through modulaton of the LACC, with $\alpha = 22 \pm 9$ Wm^{-2}.
[i]The lower limit obtained from the maximum cloud cover changes depends on systematic errors. The confidence limits are therefore meaningless.
[j]The combined PDF does not include the LGM (μ) estimate or the Phanerozoic/Clouds bounds.
[k]Using ΔT_{CRF} and μ from the Phanerozoic data instead of ΔF_{CRF} and α.

C in the absence of correlation is not *a* log$_{10}$2, but 0.) Scientifically, this is somewhat unfortunate, because without this coincidence the δ^{18}O signal would have had a clear correlation with the R_{CO2} signal, and the R_{CO2} fingerprint would have been discernible in the Phanerozoic data.

[42] If we repeat the analysis of *Shaviv and Veizer* [2003] and consider also the effects of *a* log $\Lambda(t) - \log\Omega(t)$ introduced by *Royer et al.* [2004], and corrected for R_{CO2} as described above, we obtain: C = 0.69°K (or an upper limit of 1.12, 1.42 and 1.73°K at 68%, 90% and 99% confidence levels, and a lower limit of 0.39, 0.10, −0.21°K, respectively). This gives λ = 0.28 ± 0.15°KW^{-1}m^2.

[43] Without the effect of cosmic rays (i.e., with the D term removed in the model given by equation (15)), more of the reconstructed temperature variability can be explained with CO_2, and the estimate range for λ broadens respectively to λ = 0.36 ± 0.22°KW^{-1}m^2. More limits are given in Table 1.

[44] Note that this estimate is independent of α determined in section 2. The first range for λ simply assumes that a CRF/climate link exists, while the second quoted range, even neglects this assumption. Note also that although there is no reason for the ice-volume effect on the δ^{18}O to be absent, removing it altogether would increase the estimate for λ by ≈ 0.2°KW^{-1}m^2,), i.e., just within the error bar.

3.2. CRF/ΔT Correlation Over the Phanerozoic

[45] The significant correlation between CRF and temperature over the Phanerozoic was also used to place limits on the ratio between CRF variations and temperature change. Together with the results of section 2 we can place a limit on λ.

[46] In *Shaviv and Veizer* [2003], it was found that if ΔT_{trop} is approximated with

$$\Delta T_{trop} = D[(\phi/\phi_0)^p - 1], \qquad (16)$$

where $p = 1/2$ and ϕ_0 is the CRF today, then $D = 8 \pm 4$°K. Using more data to constrain the CRF variations, model (3) of *Shaviv and Veizer* [2003] with its larger CRF variations can be ruled out, implying that D should be 5 ± 1.25°K. This can be done once the ^{10}Be-^{36}Cl exposure ages, which require calibration [*Lavielle et al.*, 1999], are considered, since these ages have intrinsically smaller errors and therefore more clustering, a higher lower limit can be placed on the CRF variations. Note also that because the galactic variations in the CRF are mostly energy independent, the CRF variations in the Iron meteorite data have the same variations as those of the higher energies responsible for the tropospheric ionization. If we generalize to other power laws p between 0.25 to 1.5, remember that $\mathcal{I} \propto \phi^{1/2}$,

and repeat the procedure described in *Shaviv and Veizer* [2003], we find that

$$\mu \equiv -\left.\frac{dT_{global}}{d\mathcal{I}}\right|_{\mathcal{I}=\mathcal{I}_0} = -2\phi_0 \left.\frac{dT_{global}}{d\phi}\right|_{\phi=\phi_0} \qquad (17)$$

$$= (2p)D\frac{\delta T_{global}}{\delta T_{trop}} = 7.5 \pm 2°\text{K}. \qquad (18)$$

The last two steps were obtained through the differentiation of equation (16) and considering that $\delta T_{global}/\delta T_{trop} \approx 1.5$ as typically obtained in GCMs [*IPCC*, 2001]. The reason the relative error does not increase much once we introduce a range of p's is because μ (but not D) is rather insensitive to p, which empirically is close to 1/2 [e.g., *Yu*, 2002; *Harrison and Aplin*, 2001; *Ermakov et al.*, 1997] (or Figure 1).

[47] Using the result for α obtained in section 2, we find $\lambda = \mu/\alpha = 0.34^{+0.25}_{-0.11}°\text{KW}^{-1}\text{m}^2$, where we quote the median λ and the 16th and 84th percentiles (1-σ). More details on the distribution appear in Figure 3 and Table 1.

3.3. Bounds From the Total T and ϕ Variations Over the Phanerozoic

[48] Using the same Phanerozoic data and an altogether different set of argumentations, we can place additional limits on λ. We do not know accurately how large are the absolute CRF variations that give rise to the temperature oscillation over the Phanerozoic. Nevertheless, we know that there is a maximum increase of $\sim$2°K in the tropical temperature above today's tropical temperature, once averaged over the 50 Ma time scale [*Veizer et al.*, 2000]. This approximately corresponds to an increase of $\Delta T \sim 3°\text{K}$ globally.

[49] Presumably, it is mostly the clouds in the clean marine environments which can be notably affected by cosmic ray flux variations, since cloud condensation nuclei are abundant over land. Thus, we assume that this temperature change could arise by removing at most the fraction of LACC which is marine. We therefore take $f_{min} \sim 80\%$ of the LACC, which would give rise to a global cooling of $f_{min}\Delta F_{LACC} \approx f_{min}$, where $\Delta F_{LACC} \approx -16.7 \text{ Wm}^{-2}$ is the total forcing of low-altitude clouds (see section 2). Namely,

$$\lambda_{min} \gtrsim \frac{\Delta T}{f_{min}\Delta F_{LACC}} \approx 0.2°\text{KW}^{-1}\text{m}^2. \qquad (19)$$

This is an absolute minimum for the climate sensitivity, otherwise, the CRF-temperature link observed over the Phanerozoic would require too large a radiative budget change to be explained by LACC variations.

3.4. Cretaceous and Eocene Climates

[50] Particular geological epochs were studied under more scrutiny, and without being averaged out on the 50 Ma time scale, as the Phanerozoic data was. In particular, there were estimates for both the radiative forcing and temperature change of two geological periods which were particularly warm relative to today. One is the Cretaceous, at about 100 Ma before present, and the second is the Eocene, at 50 Ma.

[51] *Barron et al.* [1995] estimated that the mid-Cretaceous was $7 \pm 2°\text{K}$ warmer than today, and that it arose from an increase of $8 \pm 3.5 \text{ Wm}^{-2}$ in the radiative budget. However, *Covey et al.* [1996] point out that this estimate included only the change from the increased amount of atmospheric CO_2 and it did not include the increased forcing associated with surface albedo changes. Once taken into account, the *Hoffert and Covey* [1992] estimate for the radiative forcing increases to $15.7 \pm 6.8 \text{ Wm}^{-2}$. Their estimate for the temperature increase is also larger at $9 \pm 2°\text{K}$. We adopt the *Hoffert and Covey* [1992] estimate as it appears to consider most factors affecting the radiative budget. The large error in their quoted radiative budget reflects the limited extent to which the various climate drivers can be reconstructed over geological time scales.

[52] *Covey et al.* [1996] estimated the temperature and radiative flux increases associated with the Eocene. They are $4.3 \pm 2.1°\text{K}$ and $11.8 \pm 3.6 \text{ Wm}^{-2}$, respectively. Like the Cretaceous comparison, we should also keep in mind that it is not unreasonable for unaccounted large contributions to exist.

[53] The temperature and forcings can be used to estimate the sensitivity through $\lambda = \Delta T/\Delta F$. The results for the Eocene and Cretaceous are $\lambda = 0.37^{+0.20}_{-0.16}°\text{KW}^{-1}\text{m}^2$ and $\lambda = 0.57^{+0.44}_{-0.18}°\text{KW}^{-1}\text{m}^2$, respectively. They are also summarized in Figure 2 and Table 1.

[54] These estimates do not include however the possibility that CRF variations affect climate. To estimate this effect, we estimate the CRF differences between the two geological periods and today using the CRF reconstruction described in *Shaviv* [2002b]. We then calculate ΔF_{CR} arising from the CRF change and use $\Delta T = \lambda(\Delta F_0 + \Delta F_{CR})$ to obtain λ.

[55] We find that the CRF was 20% to 60% of the flux today during the mid-Cretaceous. Through the effects on clouds, this should have contributed towards an increase in temperature, and therefore reduce our estimate for λ. During the Eocene, ϕ_{CR} should have been between 0% and 20% higher than today. From the 6 epochs described here, this is the only case in which the effect of the CRF is to increase the estimate for the climate sensitivity.

[56] The radiative forcing associated with the CRF variations can be estimated using the value of α. Numerically, we find $\Delta F_{CRF} \approx (\sqrt{1.1 \pm 0.1} - 1)\alpha = -1.1 \pm 1.2 \text{ Wm}^{-2}$ for the Eocene and $\Delta F_{CRF} \approx (\sqrt{0.2 \text{ to } 0.6} - 1)\alpha = 7.0 \pm 4 \text{ Wm}^{-2}$ for the Cretaceous. The square root arises because α is defined using changes in the CRII and we adopt $p \approx 0.5$. The new estimates are $\lambda = 0.40^{+0.25}_{-0.12}°\text{KW}^{-1}\text{m}^2$ for the Cretaceous, and $\lambda = 0.41^{+0.32}_{-0.18}°\text{KW}^{-1}\text{m}^2$ for the Eocene. (More detail is given in Figure 3 and Table 1.)

3.5. Warming Since the Last Glacial Maximum

[57] Several studies have attempted to estimate the global sensitivity by comparing the temperature increase since the last glacial maximum (LGM) with the radiative forcing change. For example, *Hoffert and Covey* [1992] estimate that a radiative forcing of $\Delta F = 6.7 \pm 0.9 \text{ Wm}^{-2}$ is reponsible for a temperature increase of $\Delta T = 3 \pm 0.6°\text{K}$. On the other hand, *Hansen et al.* [1993] find a higher sensitivity. This is because they find that a similar radiative forcing of $\Delta F = 7.1 \pm 1.5 \text{ Wm}^{-2}$ is responsible for a much larger $\Delta T = 5 \pm 1°\text{K}$ increase. The main difference is that
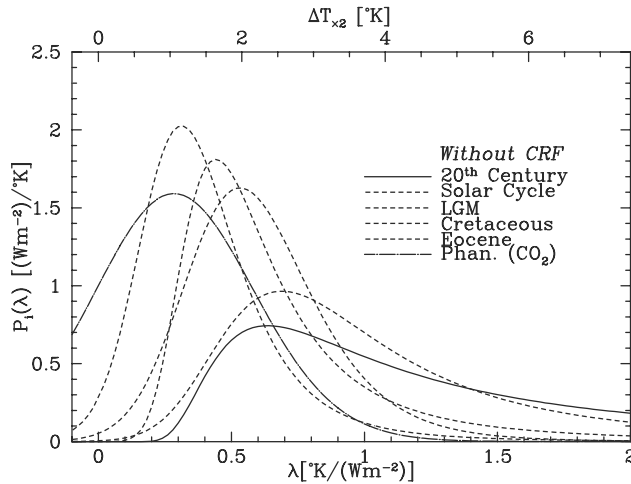
Figure 2. The probability distribution function for λ (and $\Delta T_{\times 2}$) obtained by comparing radiation budget differences to temperature change over various time scales, assuming that CRF variations do not affect the global climate (though it does includes the small solar luminosity changes). We also assume, as *Gregory et al.* [2002], that ΔT and ΔF entering λ have Gaussian errors. The cases are as follows: (1) temperature increase over the past century (following *Gregory et al.* [2002]), (2) temperature variations over 300 years of solar cycles, (3) warming since the LGM (following *Hoffert and Covey* [1992] and *Hansen et al.* [1993]), (4) cooling relative to the Cretaceous ($\sim$100 Ma [*Hoffert and Covey*, 1992]), (5) cooling relative to the Eocene ($\sim$55 Ma, following *Covey et al.* [1996]), and (6) Phanerozoic ΔT versus R_{CO2} (section 3.1, following *Shaviv and Veizer* [2003]). We assume that the temperature increase $\Delta T_{\times 2}$ following the doubling of the atmospheric CO_2 content corresponds to an increase of 3.71 Wm^{-2} [*Myhre et al.*, 1998].

Hoffert and Covey base their temperature esimate on the oceanic CLIMAP temperature reconstruction, while Hansen et al. based theirs on land temperature proxies. We will adopt the average temperature change and increase the error to be conservative. Namely, we choose $\Delta T = 4 \pm 1.5°K$. Similarly we take $\Delta F = 6.9 \pm 1.5$ Wm^{-2}. This gives $\lambda = 0.58^{+0.29}_{-0.20}°KW^{-1}m^2$ (as detailed in Figure 2 and Table 1).

[58] Again, the above estimates do not include the net radiative forcing change due to CRF modulation of the cloud cover.

[59] On this time scale, the cosmic ray flux can be obtained by first reconstructing the ^{10}Be production rates using ^{10}Be in ocean cores [*Frank et al.*, 1997; *Christl et al.*, 2003; *Sharma*, 2002] and then using the calculated relation between ^{10}Be production rate and CRF variations, arising from changes in either the solar activity or the terrestrial field [e.g., *Masarik and Beer*, 1999; *Sharma*, 2002] (or Appendix A). Since ^{10}Be resides long enough in the oceans to homogenize its fallout, ocean cores reflect the integrated ^{10}Be production (most of which takes place between 40° and 50° latitude). Moreover, ^{230}Th is generally used to correct for the variable sedimentation rates. Stacking cores from different geographic locations can further average out

local changes in the sedimentation and ^{10}Be fallout rates, and minimize possible local contaminations by ^{10}Be from continental dust.

[60] *Christl et al.* [2003] and *Frank et al.* [1997] assumed that ^{10}Be flux modulation on this time scale is primarily a result of modulation by the varying geomagnetic field. Using this flux, they derived that the geomagnetic field was about 50% its present value at 20 ka before present. Following the calculation in Appendix A, this reduced magnetic field corresponds to a $\sim$9% increase in the CRII.

[61] *Sharma* [2002] relaxed the assumption that the ^{10}Be flux modulation is predominantly terrestrial. By using independent proxies for the terrestrial field, he obtained that the field was only 30% lower than today, corresponding to a $\sim$6% increase in the high energy CRF. The rest of the ^{10}Be flux variations, were attributed to a reduced solar modulation factor $\Phi_{\odot}$ [*Masarik and Beer*, 1999], that at 20 ka was about a 1/3 of its average value of $\sim$550 MeV. Using Appendix A again, we find that the reduced solar activity and terrestrial fields were responsible to a $\sim$10% increase in the CRII. Thus, $\Delta F_{CRF} \approx 0.10\alpha$. We take this value.

[62] Since we find that a larger total radiative forcing is responsible for the same temperature change, we obtain a lower estimate, $\lambda = 0.44^{+0.21}_{-0.15}°KW^{-1}m^2$ (also detailed in Figure 3 and Table 1).

[63] Instead of using the radiative forcing through cloud cover modification, we can use our limits of μ which are not
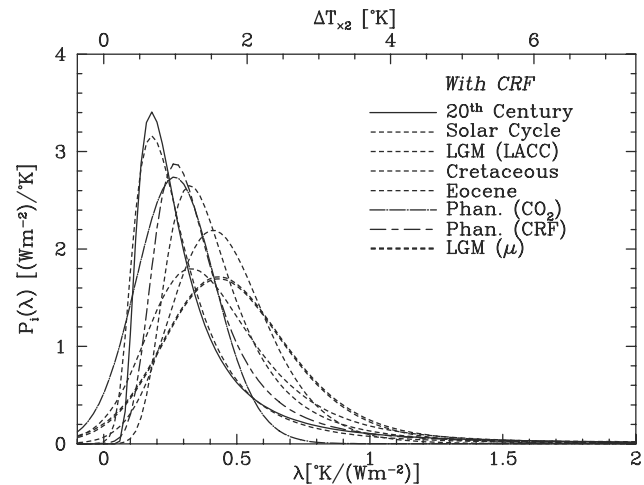

Figure 3. The probability distribution function for λ (and $\Delta T_{\times 2}$) obtained by comparing radiation budget differences to temperature change over various time scales, assuming that CRF variations do affect the global climate through modulation of the low altitude cloud cover, and that the relation between cloud cover changes and radiative forcing are given by the nominal range. The cases are the same as in Figure 2 with the added CRF effect. In addition, we have the following: (7) global sensitivity from correlation between CRF variations and temperature variations over the Phanerozoic. No equivalent for this case exists in the previous set because the CRF/climate link is required to explain this data. (8) Warming since the LGM assuming μ is given by the CRF/temperature correlation over the Phanerozoic and not necessarily through LACC variations.

based on LACC forcing, but instead on the observed temperature change over the phanerozoic. We found $\mu = 7.5 \pm 2°K$. Thus, the 10% decrease in the CRII causing low altitude tropospheric ionization should translate into a contribution of $\Delta T_{CRF} \approx 0.75$ to $0.2°K$. Next, the sensitivity relation gives $\Delta T = \lambda(\Delta F_0 + \Delta F_{CRF}) \equiv \lambda\Delta F_0 + \Delta T_{CRF}$, and thereby obtain: $\lambda = 0.48^{+0.27}_{-0.20}°KW^{-1}m^2$.

[64] To summarize, the effect of the decreased CRF since the LGM is to reduce our estimate for λ by about 20%, which is smaller than the error in the estimate itself. This result is valid also if we do not believe the CRF-climate link is through LACC moduation, but merely that such a link exists.

3.6. Warming Over the Past Century

[65] Climate sensitivity can also be estimated using the global warming observed over the past century once the radiative forcing with their uncertainties are estimated.

[66] Since the time scale is relatively short, it is necessary to consider the finite heat capacity of the oceans. We base our analysis here on the work of *Gregory et al.* [2002], who tackled this problem by considering the heat flux into the ocean in the energy budget. The main difference between our modified analysis here and that of *Gregory et al.* [2002], is that we will also consider the radiative forcing associated with the decreased CRF over the past century. Unlike the warming since the LGM, where this was a small correction, here it is will prove to be a notable one.

[67] Again, we assume that the CRF modulates the LACC and that its radiative forcing is given in section 2.

[68] *Gregory et al.* [2002] compared the period 1850–1900 with 1950–1990. Since the CRF record does not go back far enough, we need to use ^{10}Be as proxy data, which is known to be a good proxy of solar activity [e.g., *Lockwood*, 2001, 2003; *Usoskin et al.*, 2002]. Using the Dye 3 record, the average ^{10}Be flux appears to have decreased from about 1.1 to 0.7×10^4atoms g^{-1} between the former and latter periods [*Beer*, 2000; *McCracken et al.*, 2004]. Using the calculation in Appendix A, this reduction in ^{10}Be, implies a reduction of about 6% in the CRII. Using our estimate for the radiative forcing change in section 2, this corresponds to a forcing of about 1.3 ± 0.5Wm^{-2}.

[69] According to *Gregory et al.* [2002],

$$\lambda\overline{\Delta T} = \overline{F} - \overline{Q}, \qquad (20)$$

where $\overline{F}$ is the change in the radiative forcing (i.e., in the energy balance), while $\overline{Q}$ is the average net heat flux which entered the oceans between the two periods.

[70] In our modified case $\overline{F} = \overline{F}_0 + \overline{F}_{CRF}$, where $\overline{F}_0$ is the "standard" radiative forcing that was estimated by *Gregory et al.* [2002] to be $\overline{F}_0 = -0.3$ to 1 Wm^{-2}. It includes anthropogenic, volcanic, solar luminosity and aerosol contributions (with the last one contributing the largest uncertainty). $\overline{Q}$ was estimated to be 0.32 ± 0.15 Wm^{-2} while $\overline{\Delta T} = 0.335 \pm 0.033°K$ (all at 2σ).

[71] Like *Gregory et al.* [2002], we assume that the errors have a Gaussian distribution. Following their procedure, we calculate the probability distribution function (PDF) for λ. They are given in Figures 2 and 3 for the CRF and no-CRF cases. The added complication in the CRF case is the extra PDF for α, which implies that $\overline{F}_{CRF}$ has a PDF itself. The
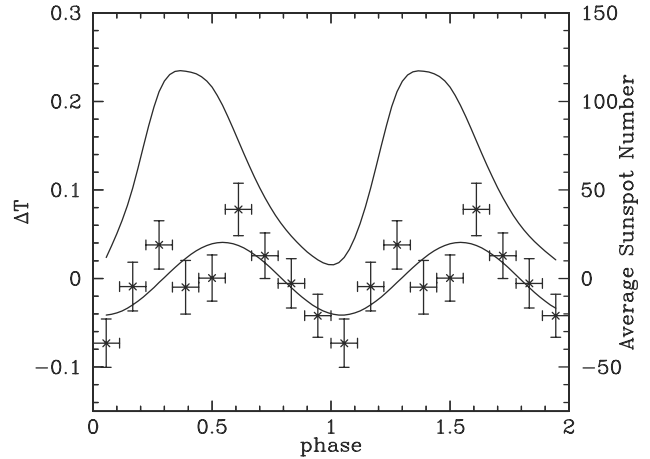

Figure 4. Plotted are average number of sunspots, the global temperature and a sinosoidal fit. The global surface temperature is the reconstructed temperature over the past 300 years (with variations on time scales longer than 30 years removed) folded over the solar cycle length. The average sunspot number folded over the same cycle.

PDF obtained for the $\overline{F}_{CRF} = 0$ case is the same as the result of *Gregory et al.* [2002].

[72] Inspection of Figure 3 and Table 1 reveals that $\lambda = 0.27^{+0.32}_{-0.10}°KW^{-1}m^2$ at 1-σ confidence. This is a clear reduction from the results of *Gregory et al.* [2002], where the lower 16th percentile for λ is $0.67°KW^{-1}m^2$ and there is no formal upper limit. (This assumes a prior that λ cannot be negative.)

3.7. Variations Over the Solar Cycle

[73] The shortest time scale we study is that of the solar cycle. Since the expected signal arising from solar variability is small (~0.1°K) looking at the recent few cycles is problematic since internal variations (such as volcanic eruptions, ENSO and other oscillations as well as simple inter-annual variations, or "internal noise") in the climate are large and can drown the solar signal. To overcome this problem, we will look at a much longer temperature record. In particular, we use the post-Little Ice age data (i.e., last 300 years) of the *Jones et al.* [1998] thousand year long reconstruction of temperature for both hemispheres, which includes proxy data of tree rings, ice cores, corals, and historical documents. The catch is that the solar cycle is not stable, and the actual period varies between about 9 and 12 years. To overcome this problem, we do not perform a harmonic analysis. Instead, we fold and average the data over the varying solar cycle period. Namely, each year is asigned a phase φ defined as the time since last sunspot minimum divided by the length of the particular cycle encompassing the given year. Once we do so, we can average all points within a phase bin and obtain the average temperature. Also, the internal variance in the temperature allows us to estimate the error in $\Delta T(\varphi)$. The result is depicted in Figure 4.

[74] Evident from the figure is the fact that the temperature has a near sinusoidal behavior. By performing a χ^2 fit to a form $\Delta T(\varphi) = \overline{\Delta T} + (a/2)\cos(2\pi(\varphi - \varphi_0))$ with φ_0 the

phase relative to the occurrence of maximum sunspot number, we find at the 1-σ confidence limit that:

$$a = 0.09 \pm 0.03°K, \qquad (21)$$

$$\varphi_0 = 1.0 \pm 0.6 \text{ rad.} \qquad (22)$$

The value of φ_0 implies that the average temperature lags behind the maximum sunspot number by 1.8 ± 1.0 years. This is to be expected, because of Earth's finite heat capacity. As a result, the response to radiative perturbations is not only damped, but it is lagged as well.

[75] Other analyses estimated the surface temperature variation over the 11-yr solar cycle. *Douglass and Clader* [2002] found $a = 0.11 \pm 0.02°K$, while *White et al.* [1997] found $a = 0.10 \pm 0.02°K$. Together with the current result, we will adopt $a = 0.10 \pm 0.02°K$ for the temperature variation between solar minimum and solar maximum.

[76] We now use the results of section 2. In particular, the above temperature variations are assumed to arise from the ∼1.6% variations observed in the LACC, such that the forcing over the solar cycle is $\Delta F_{LACC} = 1.0 \pm 0.4$ Wm^{-2}. An additional contribution of $\Delta F_{flux} = 0.35$ Wm^{-2} is due to changes in the solar flux. The sensitivity itself is then given by

$$\lambda = \frac{\Delta T / d}{\Delta F} \qquad (23)$$

where d is a damping factor which arises from the finite heat capacity of the climate system and its inability to reach equilibrium at a finite time.

[77] The value of the damping factor is not well known. In principle, it can be obtained in climate models, but these give a range of values. Using a simple ocean/climate model, M. E. Schlesinger et al. (On the use of autoregression models to estimate climate sensitivity, submitted to *Climate Change*, 2004) (hereinafter referred to as Schlesinger et al., submitted manuscript, 2004) obtained a damping of about 0.25 on the 11-yr solar cycle time scale (and about 0.75 on the centennial time scale). Other more extensive simulations find that the 11-yr solar cycle is damped relative to the centennial scale by a factor of ∼0.54 [*Cubasch et al.*, 1997], 0.33 [*Rind et al.*, 1999] or by comparing solar forcing to actual climate responce, to ∼0.68 [*Waple et al.*, 2002]. If we further consider that the centennial time scale is damped relative to the long term response, by a factor of ∼0.7−0.75 [*IPCC*, 2001; Schlesinger et al., submitted manuscript, 2004], then the 4 estimates for the damping factor are encompassed within $d = 0.35 \pm 0.15$, for periodic oscillations with an 11-yr period.

[78] Note that by resorting to GCMs for the estimate of the damping factor, we are somewhat unfaithful to the spirit of this work, which is to estimate the sensitivity independently to the usage of GCM simulations. Nevertheless, the damping we use is a characteristic describing the relative behavior of different time scales. We still avoid using the absolute sensitivity obtained in GCMs. Moreover, the analysis of *Waple et al.* [2002] does indicate that empirically, the damping factor is consistent with that obtained in
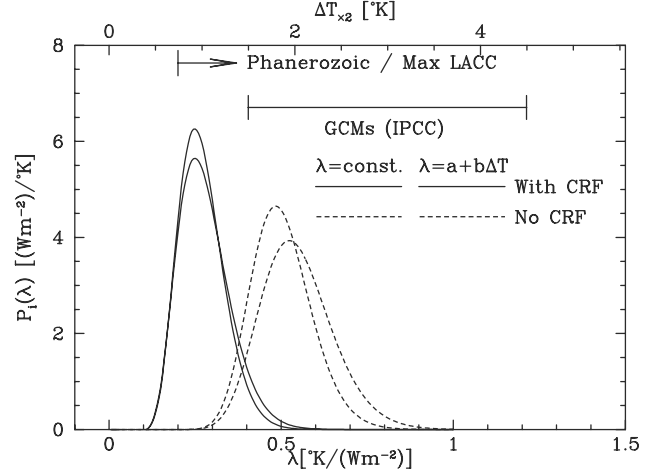

Figure 5. The combined probability distribution functions for λ obtained by combining the PDFs given in Figures 2 and 3 when the CRF/climate link is either neglected or included. (In the latter case, the combination is done as explained in the text.) Thin lines denote the result if λ is assumed to be temperature insensitive, while the heavy line is the result obtained when λ is allowed to be a linear function of the temperature. The latter case, the distribution for λ today is plotted. Also marked are the two additional constraints obtained from the Phanerozoic data which do not depend on the CRF/LACC link, as well as the sensitivity range of 1.5 to 4.5°K, which according to *IPCC* [2001] is "widely cited". Note that the sensitivity range of the 15 GCM models actually used by the *IPCC* [2001] is 2.0 to 5.1°K.

GCMs. The fact that this result is somewhat larger than GCMs on average, would imply that we maybe underestimating the damping factor, and with it, overestimating the climate sensitivity.

[79] For the above nominal values of ΔT, ΔF and d, equation (23) yields that $\lambda = 0.26^{+0.26}_{-0.11}°KW^{-1}m^2$. Without the effects of the CRF, a much larger sensitivity (of $\lambda = 0.94^{+0.91}_{-0.35}°KW^{-1}m^2$) is obtained because the same temperature variations are then to be explained only by the relatively small solar flux variations.

3.8. Combined Results

[80] We now proceed to combine the PDFs obtained in the cases described in Figure 2, when the CRF/climate link is neglected, and the cases described in Figure 3, when the CRF/LACC effect is included. We combine the results in two cases. In the first, we assume that the global temperature sensitivity is constant, namely, that it does not depend on the average terrestrial temperature. In the second case, we allow the sensitivity to be temperature dependent.

3.8.1. Constant Sensitivity

[81] When combining the results under the assumption that CRF does not introduce a radiative forcing, we can simply multiply the PDFs and renormalize the result. The reason is that the error in the estimates of all the ΔF_0 and ΔT are presumably uncorrelated with each other, and also because we have no prior on the value of λ (except perhaps that it should be positive).
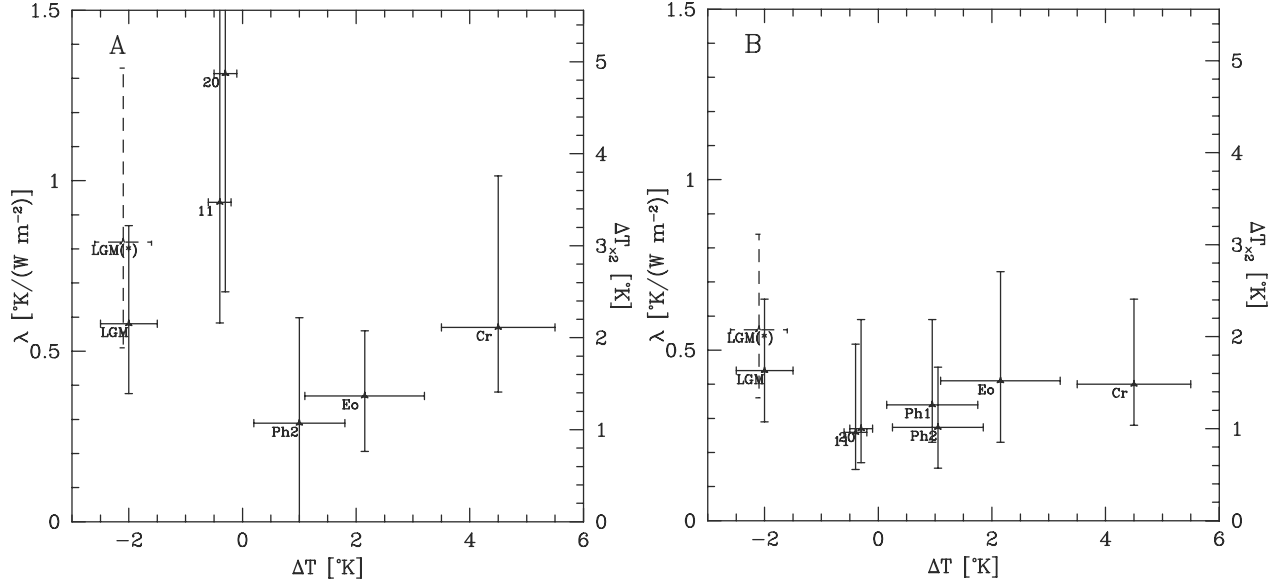
Figure 6. The estimated sensitivity λ as a function of the average temperature ΔT relative to today over which the sensitivity was calculated (e.g., average temperature between today and a given epoch if conditions at the given epoch and today are used to estimate the sensitivity). The values are for the Last Glacial Maximum (LGM), 11 year solar cycle over the past 200 years (11), 20th century global warming (20), Phanerozoic though comparison of the tropical temperature to CRF variations (Ph1) or to CO_2 variations (Ph2), Eocene (Eo) and Mid-Cretaceous (Cr). (a) Assumes that the CRF contributes no radiative forcing. (b) Assumes that the CRF does affect climate. Thus, the "Ph1" measurement is not applicable and does not appear in Figure 6a. From the figures it is evident that (1) the expectation value for λ is lower if CRF affects climate; (2) the values obtained using different paleoclimatic data are notably more consistent with each other if CRF does affect climate; (3) there is no significant trend in λ versus ΔT. The dotted bars denote the LGM sensitivity obtained if the ice-sheet albedo effect is not considered to be part of the radiative forcing (see section 4).

[82] On the other hand, when combining the cases which include the CRF/LACC effect, we must bear in mind that some of the error arises from the uncertainty in α: the relation between cloud cover changes and radiative forcing. This uncertainty enters 5 PDFs, and we cannot simply multiply them. To overcome this obstacle, we calculate the PDFs assuming a given α. Then, the combined PDF is given by

$$P_{all}(\lambda) = \frac{\int \left[\prod_{i=1}^{6} P_i(\lambda, \alpha) \right] P_\alpha(\alpha) d\alpha}{\int \left[\prod_{i=1}^{6} P_i(\lambda, \alpha) \right] P_\alpha(\alpha) d\alpha d\lambda}. \quad (24)$$

Again, this assumes that we have no prior on λ, and that besides the dependence on α, the PDFs are not in anyway correlated with each other.

[83] In Figures 5 and 7 and Table 1, we plot and describe the combined PDFs obtained in the two cases. We find that $\lambda = 0.52^{+0.10}_{-0.08} °KW^{-1}m^2$ if the CRF/climate link is neglected, and that $\lambda = 0.28^{+0.07}_{-0.05} °KW^{-1}m^2$ if the CRF/LACC link is included. Values of upper and lower limits on λ and $\Delta T_{\times 2}$ at different confidence limits are given in Table 1.

3.8.2. Variable Sensitivity

[84] We now alleviate the assumption of a constant sensitivity and allow a linear relation of the form $\lambda =$ $\lambda_0 + b\Delta T$, where λ_0 is the sensitivity today and $b = d\lambda/dT$. Because the errors are not Gaussian (the distributions are generally skewed towards higher λ's) we cannot fit $\lambda(\Delta T)$ using a simple linear least squares. Instead, we calculate

$$P_{all}(\lambda_0, b) = \frac{\int \left[\prod_{i=1}^{6} P_i(\lambda_0 + b\Delta T_i, \alpha) \right] P_\alpha(\alpha) d\alpha}{\int \left[\prod_{i=1}^{6} P_i(\lambda_0 + b\Delta T_i, \alpha) \right] P_\alpha(\alpha) d\alpha d\lambda db}, \quad (25)$$

and $P_{all}(\lambda_0) = \int P_{all}(\lambda_0, b) \, db$.

[85] Here we find that $\lambda = 0.54^{+0.12}_{-0.10} °KW^{-1}m^2$ if the CRF/climate link is neglected, and that $\lambda = 0.34^{+0.10}_{-0.08} °KW^{-1}m^2$ if the CRF/LACC link is included. Values of upper and lower limits on λ and $\Delta T_{\times 2}$ at different confidence limits are given in Table 1.

[86] This is our best estimate for the global sensitivity. It translates into a CO_2 doubling temperature change of $\Delta T_{\times 2} = 1.3 \pm 0.3°K$. With the CRF/climate effect neglected, this number is $\Delta T_{\times 2} = 2.0 \pm 0.5°K$.

[87] Another point worth mentioning is the fact that once the CRF/LACC climate link is included, the median values for λ obtained using different periods differ from each other by typically 1-σ or less, while without the CRF/climate considered, differences can be larger than 2-σ. Namely, the
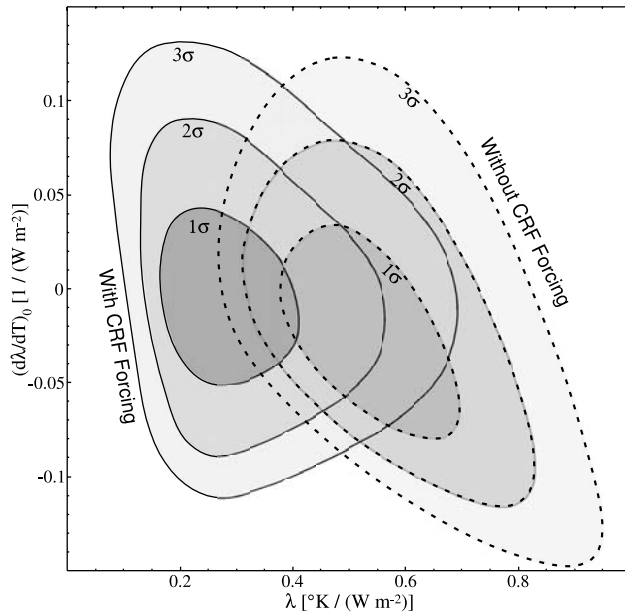
Figure 7. The two dimensional probability distribution functions for λ and its temperature sensitivity ($d\lambda/dt$), assuming the sensitivity is at most linear in the temperature. It is evident that (1) the expectation for λ is lower once the CRF/climate link is introduced; (2) in both cases, there is no clear dependence of λ on the temperature. Namely, $|d\lambda/dT| \lesssim 0.05$ $(W/m^2)^{-1}$.

CRF/climate effect markably improves the consistency of the data. This can be seen in Figure 6.

4. Discussion

[88] We compared the radiative forcing and temperature change over several different time scales, while taking into consideration the alleged link between CRF variations and temperature change. We found that the 6 different time scales can be used to place similar bound on the global climate sensitivity and, when possible, also on the quantitative relation between CRF variations and temperature change.

[89] Before continuing with a discussion of the different caveats and implications of the results obtained, we should carefully consider the meaning of the sensitivity calculated. Specifically, the sensitivity calculated was obtained through the comparison of radiative forcings to temperature response. However, in some cases, it is not clear whether a radiative forcing should be considered as part of the response of the system or part of the drivers. For the 11-yr solar cycle and the Phanerozoic-$\Delta T/\Delta\phi$ comparisons, it is clear we are considering only "external" forcings and everything terrestrial is part of the system. In the Phanerozoic-$\Delta T/CO_2$ and 20th century warming, the "external" drivers also include variation in the greenhouse gasses (excluding water vapor). We explicitly assumed that they are not part of the system but are externally forced, for example, through tectonic activity in the geological case or anthropogenic over the 20th century.

[90] The case of the LGM comparison, and to a notably smaller extent, the Cretaceous and Eocene comparisons,

include changes associated with changes in the extent of the ice-sheets. In principle, these can be considered as external drivers or as an integral part of the system. In the LGM calculation, for example, the LGM radiative forcing of $7 Wm^{-2}$ [*Hansen et al.*, 1993] we used, includes about $2 Wm^{-2}$ due to ice-sheet albedo effects. If we allow the ice-sheet changes to be part of the response of the system, then the sensitivity obtained from the LGM is notably higher, being $\lambda = 0.56^{+0.28}_{-0.20} {}^\circ KW^{-1}m^2$. Thus, the sensitivity we used in the analysis does not include the response of the cryosphere. For cold climates (i.e., colder than today) we would underestimate the sensitivity if the cryosphere is allowed to be part of the system.

[91] Other than the important point above, we should also keep in mind that different time scales and methods suffer from different uncertainties. These include the following:

[92] 1. Limits based on the geochemical record over the past 550 million years implicitly assume that estimates of temperature variations using $\delta^{18}O$ is well known. In principle, various biases might distort this relation and produce a wrong temperature scale.

[93] 2. Perhaps the largest caveat is the possibility that different average climate conditions have different sensitivities (e.g., due to changed geography, changes in the cryosphere, or large scale atmospheric and oceanic flows). Nevertheless, the fact that about half a dozen independent analyses based on paleoclimatic to recent data yield roughly the same sensitivity should indicate that we are probably not missing large radiative forcing terms. Otherwise, there is no reason, other than chance, to obtain results consistent with each other. Moreover, to partially address this point, we allowed for λ to be a linear function of temperature, but found no significant dependence (Figure 7).

[94] 3. Most of the estimates of the climate sensitivity assume the CRF/climate link is through modification of the LACC and that the radiative forcing associated with it is known. This entails in it several assumptions: (1) That LACC changes observed by the ISCCP measurements, for example, are indeed well represented by changes in the amount of cloud cover as opposed to other cloud characteristics. (2) That the incremental cloud cover changes behave as the average. (3) That tropospheric ionization does not markably affect the global temperature through an effect not related to cloud cover modifications. These uncertainties will not be resolved without detailed understanding of how and to what extent does atmospheric ionization affects the formation of cloud condensation nuclei, which affect cloud cover. Nevertheless, the value of the sensitivity could still be independently bracketed using argumentation which does not assume the relation is through the LACC variations.

[95] 4. Over the short time scales associated with the solar cycle, one of the main uncertainties is the damping factor in the effect of a changed radiative forcing.

[96] 5. The analysis implicitly assumes that internal variations, with el-niño being the best example, are averaged out. This is required because we are interested in the equilibrium response of the average climate system. In the case of the Phanerozoic and the 11-yr comparisons, this is implicitly considered because we only consider the part of the temperature variations that changed in sync with the

radiative forcing. Thus, by definition, internal oscillations or randomness are averaged out. The 20th century warming follows the analysis of *Gregory et al.* [2002], who decoupled the atmospheric from the oceanic components by explicitly considering the heat transfer to the oceans. Since the atmosphere is not expected to have internal dynamics (without external forcing) on this time scale, all such internal contributions are presumably averaged out. The three other comparisons are the climate variations since the mid-Cretaceous, the Eocene and the LGM. Here random or oscillatory long term internal variations of the system could in principle exist and possibly affect the sensitivity estimate.

[97] 6. We implicitly assumed here that climate sensitivity to changes in the cosmic ray flux remained constant throughout the ages, under varying climatic and geographic conditions. This, however, is not automatically guaranteed, since the link was calibrated under Holocene conditions. Over time, for example, there could have been a change in the average amount of water vapor in the atmosphere, governed by the average temperature, or the fraction and geographic distribution of the landmass from which CCN that are unrelated to atmospheric ionization, can originate. Thus, it is not unreasonable for there to have been variations in the quantitative link between CRF variations and changes to the radiation budget. Without a better understanding of the physical mechanism governing the link, this assumption should therefore only be considered as a working hypothesis.

[98] 7. In the analysis, the sensitivity was obtained either by considering small "perturbations" around Holocene type conditions, or, through comparison of largely different climates. Thus, it is not unlikely that we are missing climate instabilities which arise when considering small variations around average conditions different than today. As an illustration, a prominent ocean current like the gulf stream could switch on or off around average conditions different than today. Not only would our estimate for λ be wrong in this case, the system may have complicated nonlinear dynamics that cannot even be described with an effective λ, such as a memory effect (e.g., hysteresis).

[99] Having listed the caveats, it should also be noted that once the CRF/climate effect is taken into account, an agreement between the sensitivities obtained. Not only does it indicate that we are probably not missing unaccounted factors, it provides another indicator that the CRF/climate effect is real (see Figure 6a versus Figure 6b).

[100] Our best estimate is $\Delta T_{\times 2} \approx 1.3 \pm 0.3°K$. This is at the lower end of the often quoted range of $\Delta T_{\times 2} = 1.5$ to $4.5°K$ [*IPCC*, 2001] obtained from Global Circulation Models (GCMs). *Cess et al.* [1989] have shown that the climate sensitivity obtained in this type of simulations predominantly depends on how clouds are treated, and whether they contribute a positive or negative feedback. The models roughly give that $\lambda^{-1} \approx 2.2$ Wm^{-2}/°K $- \Delta F_{cloud}/\Delta \bar{T}$ with ΔF_{cloud} being the feedback forcing of clouds associated with a temperature change of $\Delta \bar{T}$. Thus, for a GCM to be compatible with the results obtained here, a negative cloud feedback is required. One such example was suggested by *Lindzen et al.* [2001].

[101] On the other side of the coin, we can also rule out very small climate sensitivities. This can be used for example to place a limit on possible large negative feedbacks, or to a lower limit on the effect of anthropogenic greenhouse gas (GHG) warming.

[102] Since the beginning of the industrial era ($\sim$1750), non-solar sources contributed a net forcing of 0.85 ± 1.3 Wm^{-2} [*IPCC*, 2001] (assuming the errors are Gaussian). Over the past century alone, this number is 0.5 ± 1.3 Wm^{-2}. The main reason why the error is large is because of the uncertain "indirect" contribution of aerosols, namely, their effect on cloud cover. It is currently estimated to be in the range -1 ± 1 Wm^{-2} [*IPCC*, 2001]. Thus, anthropogenic sources alone contributed to a warming of $0.14 \pm 0.36°K$ since the beginning of the 20th century.

[103] The sensitivity result can also be used to estimate the solar contribution towards global warming. Over the past century, the increased solar activity has been responsible for a stronger solar wind and a lower CRF. Using results of section 3.6, the reduced ionization and LACC were responsible for an increased radiative forcing of 1.3 ± 0.5 Wm^{-2}. In addition, the globally averaged solar luminosity increased by about 0.4 ± 0.1 Wm^{-2} according to *Solanki and Fligge* [1998], *Hoyt and Schatten* [1993], and *Lean et al.* [1995]. Thus, increased solar activity is responsible for a total increase of 1.7 ± 0.6 Wm^{-2}. Using our estimate for λ, we find $\Delta T_{solar} = 0.47 \pm 0.19°K$.

[104] We therefore find that the combined solar and anthropogenic sources were responsible for an increase of $0.61 \pm 0.42°K$. This should be compared with the observed $0.57 \pm 0.17°K$ increase in global surface temperature [*IPCC*, 2001]. In other words, the result we find for the sensitivity and drivers are consistent with the observed temperature increase. This conclusion, about the relative role of solar versus anthropogenic sources was independently reached by comparing the non-monotonic temperature increase with the non-monotonic solar activity increase and the monotonic increase in GHGs [*Soon et al.*, 1996b].

Appendix A

[105] Over geological time scales, both a galactic cosmic ray diffusion model and a record in Iron meteorites can be independently used to estimate CRF and atmospheric ionization rate changes. On shorter time scales, of a few 100 ka or shorter, we need another method. ^{10}Be is sensitive to the varying CRF and can be reconstructed using ice-cores and sea floor sediments. However, the energy sensitivity is different than that of atmospheric ionization: ^{10}Be is formed by CRs which are on average less energetic than the CRs responsible for the atmospheric ionization. Thus, using the ^{10}Be record to reconstruct the atmospheric ionization is possible but it requires correcting for the different energy sensitivity.

[106] We calculate here the sensitivity of the atmospheric ionization rate to changes in the CRs which arise from changes in solar activity (as encompassed in the solar modulation parameter $\Phi_{\odot}$) and changes in the terrestrial magnetic field strength m as compared to the field today. We will compare those to the production rate of ^{10}Be as a function of both parameters.
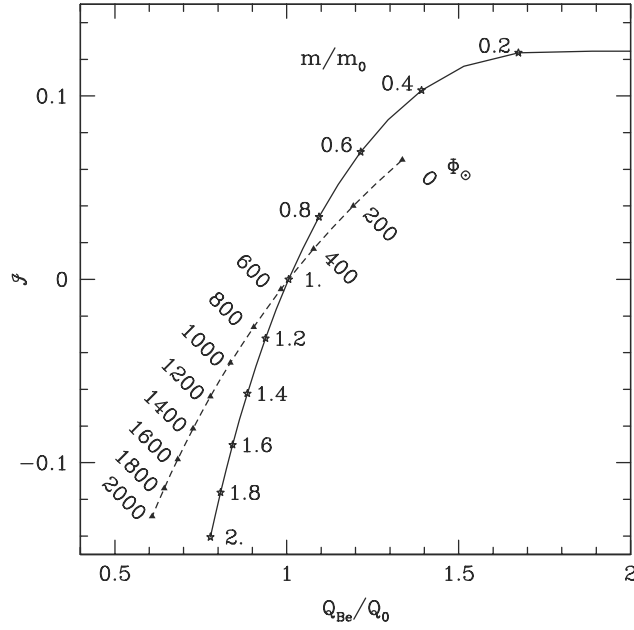
Figure A1. Calculated relation between the relative change in the average global cosmic ray induced ionization ($\mathcal{I}$) and the relative change Q_{Be}/Q_0 in the ^{10}Be production. The two curves denote the relations obtained when the terrestrial magnetic field m is changed relative to today's average value m_0 (solid line) while assuming $\Phi_\odot = 550$ MeV, and when the solar modulation parameter $\Phi_\odot$ (in MeV) is changed (dashed line) while assuming $m = m_0$.

[107] The flux of cosmic rays reaching 1 AU depends on the solar modulation parameter. It is given by [*Masarik and Beer*, 1999]:

$$J(E, \Phi_\odot) = C_p \frac{E_p(E_p + 2m_pc^2)(E_p + x + \Phi_\odot)^{-2.5}}{(E_p + \Phi_\odot)(E_p + 2m_pc^2 + \Phi_\odot)}, \quad (A1)$$

with $x = (780 \text{ MeV}) \exp(-2.5 \times 10^{-4}E_p/\text{MeV})$ and $C = 1.24 \times 10^6$ cm^{-2} s^{-1}MeV^{-1}. Frfsom these cosmic rays, the particles which can actually reach the atmosphere and not be cut off by the magnetic field, at latitude ϑ, are those with a rigidity above the cutoff, given by

$$P_c(\vartheta) \approx (14.8\text{GV}) \cos^4(\vartheta)(m/m_0), \quad (A2)$$

where m is the geomagnetic dipole moment, and $m_0 = 7.8 \times 10^{25}$ G cm^3 is the current day dipole.

[108] *Masarik and Beer* [1999] used these expressions and the various spallation cross-sections to obtain the globally averaged production rate of ^{10}Be as a function of $\Phi_\odot$ and m. Their results were analytically fitted by *Sharma* [2002]. Thus, given changes in $\Phi_\odot$ and m, relative to their recent averages, the change in the ^{10}Be production rate can be straightforwardly obtained.

[109] The next step is to use the ionization yield to obtain to total ionization rate from the flux which can actually reach the atmosphere. We use the ionization yields calculated by *Usoskin et al.* [2004b]. These are given as $Y(E, h)$, the total ionization at height h arising from a cosmic ray at

energy E. We take the average ionization between 0 and 3 km, the altitude of LACC.

[110] To obtain the actual ionization rate R, we integrate:

$$R(m, \Phi_\odot; \vartheta) = \int_{P_c}^\infty J(E, \Phi_\odot)Y(E, \vartheta)dE. \quad (A3)$$

[111] Empirically, it appears that cloud cover is proportional to the density of atmospheric ions [*Usoskin et al.*, 2004a], while the latter is proportional to the relative change in $\sqrt{I(m, \Phi_\odot; \vartheta)}$ in the lower parts of the atmosphere because of ion-ion recombination [*Yu*, 2002; *Harrison and Aplin*, 2001; *Ermakov et al.*, 1997] i.e., $p \approx 1/2$ (in equation (16)).

[112] Thus, we can integrate over latitude and obtain the average global variation in the relative change of cosmic ray induced ions $\mathcal{I}$,

$$\mathcal{I} = \frac{1}{2} \int \left[\left(\frac{R(m, \Phi_\odot; \vartheta)}{R(m_0, \bar{\Phi}_\odot; \vartheta)} \right)^{1/2} - 1 \right] \cos\vartheta d\vartheta, \quad (A4)$$

where $\bar{\Phi}_\odot = 550$ MeV is the long term average of $\Phi_\odot$. If the actual value of p is somewhat different from 1/2, then $\delta(LACC) = (2p)\,\mathcal{I}$ (Figure A1).

References

Ardanuy, P. E., L. L. Stowe, A. Gruber, and M. Weiss (1991), Shortwave, longwave, and net cloud-radiative forcing as determined from Nimbus-7 observations, *J. Geophys. Res.*, *96*(D10), 18,537–18,549.

Barron, E. J., P. J. Fawcett, W. H. Peterson, D. Pollard, and S. L. Thompson (1995), A simulation of midcretaceous climate, *Paleoceanography*, *10*(5), 953–962.

Beer, J. (2000), Long-term indirect indices of solar variability, *Space Sci. Rev.*, *94*, 53–66.

Beer, J., W. Mende, and R. Stellmacher (2000), The role of the sun in cllimate forcing, *Quat. Sci. Rev.*, *19*, 403–415.

Berner, R. A., and Z. Kothavala (2001), GEOCARB III: Revised model of atmospheric CO$_2$ over Phanerozoic time, *Am. J. Sci.*, *301*, 182–204.

Carslaw, K. S., R. G. Harrison, and J. Kirkby (2002), Cosmic rays, clouds, and climate, *Science*, *298*, 1732–1737.

Cess, R. D., et al. (1989), Interpretation of cloud-climate feedback as produced by 14 atmospheric general-circulation models, *Science*, *245*(4917), 513–516.

Christl, M., C. Strobl, and A. Mangini (2003), Beryllium-10 in deep-sea sediments: A tracer for the Earth's magnetic field intensity during the last 200,000 years, *Quat. Sci. Rev.*, *22*, 725–739.

Covey, C., L. C. Sloan, and M. I. Hoffert (1996), Paleoclimate data constraints on climate sensitivity: The paleocalibration method, *Clim. Change*, *32*(2), 165–184.

Cubasch, U., R. Voss, G. C. Hegerl, J. Waszkewitz, and T. J. Crowley (1997), Simulation of the influence of solar radiation variations on the global climate with an ocean-atmosphere general circulation model, *Clim. Dyn.*, *13*(11), 757–767.

Douglass, D. H., and B. D. Clader (2002), Climate sensitivity of the earth to solar irradiance, *Geophys. Res. Lett.*, *29*(16), 1786, doi:10.1029/2002GL015345.

Eddy, J. (1976), The mounder minimum, *Science*, *192*, 1189–1202.

Eichkorn, S., S. Wilhelm, H. Aufmhoff, K. H. Wohlfrom, and F. Arnold (2002), Cosmic ray-induced aerosol formation: First observational evidence from aircraft based ion mass spectrometer measurements in the upper troposphere, *Geophys. Res. Lett.*, *29*(14), 1698, doi:10.1029/2002GL015044.

Ermakov, V. I., G. A. Bazilevskaya, P. E. Pokrevsky, and Y. I. Stozhkov (1997), Ion balance equation in the atmosphere, *J. Geophys. Res.*, *102*, 23,413–23,420.

Farrar, P. D. (2000), Are cosmic rays influencing oceanic cloud coverage - or is it only El Nino?, *Clim. Change*, *47*(1–2), 7–15.

Frank, M., B. Schwarz, S. Baumann, P. W. Kubik, M. Suter, and A. Mangini (1997), A 200 kyr record of cosmogenic radionuclide production rate and geomagnetic field intensity from Be-10 in globally stacked deep-sea sediments, *Earth Planet. Sci. Lett.*, *149*, 121–129.

Friis-Christensen, E., and K. Lassen (1991), Length of the solar cycle: An indicator of solar activity closely associated with climate, *Science*, *254*, 698.

Frohlich, C., and J. Lean (1998), The sun's total irradiance: Cycles, trends and related climate change uncertainties since 1976, *Geophys. Res. Lett.*, *25*(23), 4377–4380.

Gregory, J. M., R. J. Stouffer, S. C. B. Raper, P. A. Stott, and N. A. Rayner (2002), An observationally based estimate of the climate sensitivity, *J. Clim.*, *15*, 3117–3121.

Hansen, J., A. Lacis, R. Ruedy, M. Sato, and H. Wilson (1993), How sensitive is the worlds climate, *Res. Explor.*, *9*(2), 142–158.

Hansen, J. E., M. Sato, A. Lacis, R. Ruedy, I. Tegen, and E. Matthews (1998), Climate forcings in the industrial era, *Proc. Natl. Acad. Sci.*, *95*, 12,753–12,758.

Harrison, R. G., and K. L. Aplin (2001), Atmospheric condensation nuclei formation and high-energy radiation, *J. Atmos. Terr. Phys.*, *63*, 1811–1819.

Hartmann, D. L., M. E. Ockert-Bell, and M. L. Michelsen (1992), The effect of cloud type on Earth's energy balance: Global analysis, *J. Clim.*, *5*, 128.

Herschel, W. (1796), Some remarks on the stability of the light of the sun, *Philos. Trans. R. Soc. London*, *0*, 166.

Hobbs, P. (1993), Aerosol-cloud interactions, in *Aerosol-Cloud-Climate Interactions.*, *Int. Geophys. Ser.*, vol. 54, Elsevier, New York.

Hodell, D. A., M. Brenner, J. H. Curtis, and T. Guilderson (2001), Solar forcing of drought frequency in the maya lowlands, *Science*, *292*, 1367–1370.

Hoffert, M. I., and C. Covey (1992), Deriving global climate sensitivity from paleoclimate reconstructions, *Nature*, *360*(6404), 573–576.

Hoyt, D. V., and K. H. Schatten (1993), A discussion of plausible solar irradiance variations, 1700–1992, *J. Geophys. Res.*, *98*(A11), 18,895–18,906.

Intergovernmental Panel on Climate Change (IPCC) (2001), *Climate Change 2001*, Cambridge Univ. Press, New York.

Jones, P. D., K. R. Briffa, T. P. Barnett, and S. F. B. Tett (1998), High-resolution palaeoclimatic records for the last millennium: Interpretation, integration and comparison with general circulation model control-run temperatures, *Holocene*, *8*(4), 455–471.

Kirkby, J., and A. Laaksonen (2000), Solar Variability and Clouds - Discussion Session 3c, *Space Sci. Rev.*, *94*, 397–409.

Labitzke, K., and H. van Loon (1992), *J. Clim*, *5*, 240.

Lavielle, B., K. Marti, J. Jeannot, K. Nishiizumi, and M. Caffee (1999), The ^{36}Cl-^{36}Ar-^{40}K-^{41}K records and cosmic ray production rates in iron meteorites, *Earth Planet. Sci. Lett.*, *170*, 93–104.

Lean, J., J. Beer, and R. Bradley (1995), Reconstruction of solar irradiance since 1610 - Implications for climate change, *Geophys. Res. Lett.*, *22*(23), 3195–3198.

Lindzen, R. S., M.-D. Chou, and A. Y. Hou (2001), Does the Earth have an adaptive infrared iris?, *Bull. Am. Meteorol. Soc.*, *82*, 417–431.

Lockwood, M. (2001), Long-term variations in the magnetic fields of the Sun and the heliosphere: Their origin, effects, and implications, *J. Geophys. Res.*, *106*(A8), 16,021.

Lockwood, M. (2003), Twenty-three cycles of changing open solar magnetic flux, *J. Geophys. Res.*, *108*(A3), 1128, doi:10.1029/2002JA009431.

Marsden, D., and R. E. Lingenfelter (2003), Solar activity and cloud opacity variations: A modulated cosmic ray ionization model, *J. Atmos. Sci.*, *60*(4), 626–636.

Marsh, N., and H. Svensmark (2000a), Cosmic rays, clouds, and climate, *Space Sci. Rev.*, *94*, 215–230.

Marsh, N., and H. Svensmark (2000b), Low cloud properties influenced by cosmic rays, *Phys. Rev. Lett.*, *85*, 5004–5007.

Marsh, N., and H. Svensmark (2003), Galactic cosmic ray and El Nino–Southern Oscillation trends in International Satellite Cloud Climatology Project D2 low-cloud properties, *J. Geophys. Res.*, *108*(D6), 4195, doi:10.1029/2001JD001264.

Masarik, J., and J. Beer (1999), Simulation of particle fluxes and cosmogenic nuclide production in the Earth's atmosphere, *J. Geophys. Res.*, *104*, 12,099–12,111.

McCracken, K. G., J. Beer, and F. B. McDonald (2004), Variations in the cosmic radiation, 1890–1986, and the solar and terrestrial implications, *Adv. Space Res.*, *34*, 397–406.

Myhre, G., E. J. Highwood, K. P. Shine, and F. Stordal (1998), New estimates of radiative forcing due to well mixed greenhouse gases, *Geophys. Res. Lett.*, *25*, 2715.

Neff, U., S. J. Burns, A. Mangnini, M. Mudelsee, D. Fleitmann, and A. Matter (2001), Strong coherence between solar variability and the monsoon in oman between 9 and 6 kyr ago, *Nature*, *411*, 290–293.

Ney, E. P. (1959), Cosmic radiation and weather, *Nature*, *183*, 451.

Palle Bago, E., and J. Butler (2000), The influence of cosmic terrestrial clouds and global warming, *Astron. Geophys.*, *41*, 18–22.

Rind, D., J. Lean, and R. Healy (1999), Simulated time-dependent climate response to solar radiative forcing since 1600, *J. Geophys. Res.*, *104*(D2), 1973–1990.

Rosenfeld, D. (2000), Suppression of rain and snow by urban and industrial air pollution, *Science*, *287*, 1793–1796.

Royer, D., R. Berner, I. Montanez, N. Tabor, and D. Beerling (2004), CO_2 as a primary driver of phanerozoic climate, *GSA Today*, *14*(3), 4–10.

Sharma, M. (2002), Variations in solar magnetic activity during the last 200,000 years: Is there a sun-climate connection?, *Earth Planet. Sci. Lett.*, *199*(3–4), 459–472.

Shaviv, N. J. (2002a), Cosmic ray diffusion from the galactic spiral arms, iron meteorites, and a possible climatic connection?, *Phys. Rev. Lett.*, *89*, 051,102.

Shaviv, N. J. (2002b), The spiral structure of the Milky Way, cosmic rays, and ice age epochs on earth, *New Astron.*, *8*, 39–77.

Shaviv, N. J. (2003), Toward a solution to the early faint Sun paradox: A lower cosmic ray flux from a stronger solar wind, *J. Geophys. Res.*, *108*(A12), 1437, doi:10.1029/2003JA009997.

Shaviv, N. J., and J. Veizer (2003), A celestial driver of phanerozoic climate?, *GSA Today*, *13*(7), 4–11.

Shaviv, N., and J. Veizer (2004), Reply to Royer et al.'s letter "CO_2 as a primary driver of phanerozoic climate", *GSA Today*, *14*(7), 18.

Solanki, S. K., and M. Flligge (1998), Solar irradiance since 1874 revisited, *Geophys. Res. Lett.*, *25*(3), 341–344.

Soon, W. H., E. S. Posmentier, and S. L. Baliunas (1996a), Inference of solar irradiance variability from terrestrial temperature changes, 1880–1993: An astrophysical application of the Sun-climate connection, *Astrophys. J.*, *472*, 891.

Soon, W. H., E. S. Posmentier, and S. L. Baliunas (1996b), Inference of solar irradiance variability from terrestrial temperature changes, 1880–1993: An astrophysical application of the Sun-climate connection, *Astrophys. J.*, *472*, 891.

Soon, W. H., E. S. Posmentier, and S. L. Baliunas (2000), Climate hypersensitivity to solar forcing?, *Ann. Geophys.*, *18*, 583+.

Stephens, G. L. (1978), Radiation profiles in extended water clouds. 2. Parameterization schemes, *J. Atmos. Sci.*, *35*(11), 2123–2132.

Svensmark, H. (1998), Influence of cosmic rays on earth's climate, *Phys. Rev. Lett.*, *81*, 5027–5030.

Svensmark, H. (2000), Cosmic rays and earth's climate, *Space Sci. Rev.*, *93*, 175–185.

Twomey, S. (1977), The influence of pollution on the shortwave albedo of clouds, *J. Atmos. Sci.*, *34*, 1149–1152.

Usoskin, I. G., K. Mursula, S. K. Solanki, M. Schüssler, and G. A. Kovaltsov (2002), A physical reconstruction of cosmic ray intensity since 1610, *J. Geophys. Res.*, *107*(A11), 1374, doi:10.1029/2002JA009343.

Usoskin, I. G., N. Marsh, G. A. Kovaltsov, K. Mursula, and O. G. Gladysheva (2004a), Latitudinal dependence of low cloud amount on cosmic ray induced ionization, *Geophys. Res. Lett.*, *31*, L16109, doi:10.1029/2004GL019507.

Usoskin, I. G., O. G. Gladysheva, and G. A. Kovaltsov (2004b), Cosmic ray-induced ionization in the atmosphere: Spatial and temporal changes, *J. Atmos. Terr. Phys.*, *66*, 1791–1796, doi:10.1016/j.jastp.2004.07.037.

Veizer, J., Y. Godderis, and L. M. Francois (2000), Evidence for decoupling of atmospheric CO_2 and global climate during the phanerozoic eon, *Nature*, *408*, 698.

Waple, A. M., M. E. Mann, and R. S. Bradley (2002), Long-term patterns of solar irradiance forcing in model experiments and proxy based surface temperature reconstructions, *Clim. Dyn.*, *18*(7), 563–578.

White, W. B., J. Lean, D. R. Cayan, and M. D. Dettinger (1997), Response of global upper ocean temperature to changing solar irradiance, *J. Geophys. Res.*, *102*(C2), 3255–3266.

Yu, F. (2002), Altitude variations of cosmic ray induced production of aerosols: Implications for global cloudiness and climate, *J. Geophys. Res.*, *107*(A7), 1118, doi:10.1029/2001JA000248.

———————————

N. J. Shaviv, Racah Institute of Physics, Hebrew University of Jerusalem, Jerusalem, 91904, Israel. (shaviv@phys.huji.ac.il)